Formation of nanostructures in commercial-purity titanium via cryorolling

S.V. Zherebtsov [a,*], G.S. Dyakonov [a], A.A. Salem [b,c], V.I. Sokolenko [d], G.A. Salishchev [a], S.L. Semiatin [b]

[a] *Laboratory of Bulk Nanostructured Materials, Belgorod State University, Pobeda 85, Belgorod 308015, Russia*
[b] *Air Force Research Laboratory, Materials & Manufacturing Directorate, Wright-Patterson Air Force Base, OH 45433-7817, USA*
[c] *Universal Technology Corporation, Dayton, OH 45432, USA*
[d] *National Science Center, Kharkov Institute of Physics and Technology, Akademicheskaya-1, Kharkov 61108, Ukraine*

Abstract

Microstructure evolution in commercial-purity titanium during plane-strain multipass rolling to a true thickness strain of 2.66 at 77 and 293 K was quantified. Deformation at both temperatures was accompanied by twinning. At 77 K, twinning was more extensive in terms of the fraction of twinned grains and the duration of the twinning stage. Rolling to a true thickness strain of 2.66 resulted in the formation of a microstructure with a grain/subgrain size of ~80 nm at 77 K or ~200 nm at 293 K. The contribution of various mechanisms to the strength of titanium following rolling at 77 and 293 K was analyzed quantitatively.

Keywords: Titanium; Cryorolling; Twinning; Microstructure formation; Nanostructure

1. Introduction

The formation of a nanocrystalline microstructure in metallic materials can result in a considerable improvement in mechanical properties, such as strength and fatigue resistance [1,2]. The most common approach to produce bulk nanostructured materials is based on large (or severe) deformation at low temperature by means of methods such as high-pressure torsion [3], equal channel angular extrusion [4], accumulative roll bonding [5], twist extrusion [6] and multiaxial deformation [7].

The evolution of severely strained microstructures has been the subject of a number of efforts focused primarily on cubic materials [8–12]. In such cases, microstructure refinement during large deformation is associated with the creation of deformation-induced boundaries [8,10,12], including (i) geometrically necessary boundaries (GNBs), which separate regions that deform by different combinations of slip systems, and (ii) incidental dislocation boundaries, consisting of ordinary cell boundaries that form by the trapping of glide dislocations. The formation of GNBs with moderate-to-high misorientation requires a relatively high level of strain [8].

At ambient temperature, pure titanium (having a hexagonal crystal structure) has only four independent deformation modes involving basal or prismatic slip along the $\boldsymbol{a}$ Burgers vector in the basal plane. Therefore, tension or compression along the $\boldsymbol{c}$ axis of titanium crystals must be accommodated by twinning and/or $\boldsymbol{c}+\boldsymbol{a}$ pyramidal slip. As one of the main deformation modes, twinning in titanium typically occurs and is most readily observed during the early stages of deformation; however, it may also occur at intermediate and high levels of deformation as well. Being high-angle in nature, twin boundaries transform from well-defined coincident-site-lattice-type boundaries into arbitrary ones due to subsequent interaction with lat-

* Corresponding author. Tel./fax: +7 4722 585416.
E-mail addresses: zherebtsov@bsu.edu.ru, ser_z@mail.ru (S.V. Zherebtsov).

tice dislocations [13], thereby refining the microstructure considerably. Twin boundaries can have a marked influence on the evolution/refinement of microstructure during further straining, i.e. following the saturation of twinning. However, the nature of such microstructure evolution has been investigated to only a limited extent [10,14,15].

Prior work has suggested that twinning is one of the main factors enabling the formation of a very fine microstructure in commercial-purity (CP) titanium [14–16]. For example, a microstructure with a grain size of 100–200 nm was attained during plane-strain rolling at room temperature (RT) to a true thickness strain $\varepsilon_{th} \approx 2.6$ [15]. Microstructure evolution in CP titanium during such cold rolling was found to be associated with twinning at the initial stage of deformation and then the formation of deformation-induced high-angle boundaries [15]. In the present work, specimens of CP Ti were rolled at room and liquid nitrogen temperatures to (i) establish the effect of temperature on twinning and the degree of microstructure refinement via cryogenic processing and (ii) gain insight into the effect of twinning on microstructure refinement at large strain.

2. Materials and methods

The material for the present investigation comprised a 4 mm thick plate of CP titanium (impurities in wt.% less than: 0.18 Fe, 0.1 Si, 0.07 C, 0.04 N, 0.01 H, 0.12 O). In the as-received condition, the plate had a homogeneous, equiaxed microstructure, with an average grain size of 15 μm. All experiments were performed on material in the as-received condition.

To determine the effect of temperature and the degree of deformation on microstructure evolution, rectangular samples measuring $4 \times 10 \times 30\ mm^3$ were rolled at room (293 K) and liquid nitrogen (77 K) temperatures using a fixed rolling speed of $30\ mm\ s^{-1}$. Unidirectional multipass rolling to a total thickness strain between ~0.05 and ~2.6 was performed at both temperatures using a reduction (draft) per pass of ~0.2–0.07 mm.

Prior to cryorolling, each preform was encapsulated between sacrificial titanium sheets which were joined by spot welding. The pack was then cooled to 77 K in liquid nitrogen and rolled between room-temperature rolls. The temperature of the canned workpiece during such a pack-rolling process did not increase by more than 20 °C. To ensure nearly isothermal deformation, each pack was cooled in liquid nitrogen between each rolling pass.

The microstructure at the mid-thickness rolling plane of each deformed sample was determined using light microscopy, transmission electron microscopy (TEM) and electron backscatter diffraction (EBSD). TEM was done in a JEOL JEM-2100FX microscope. The dislocation density was determined by counting the individual dislocations within the grains/subgrains using at least six arbitrarily selected TEM images for each sample. The terms "grain", "subgrain" and "cell" were defined using the standard convention, i.e. crystallites surrounded by mainly high-angle (misorientation above 15°), low-angle (2–15°) or loose dislocation boundaries (less than 2°), respectively. The misorientation of selected boundaries was also evaluated using a single-reflection method [17]. This method is based on the direct determination of the laboratory coordinates of the normal relative to the reflecting plane. The procedure consists of obtaining at least two (preferably three) diffraction spots (reflections) of different planes at different goniometer angles. The best reflecting positions correspond to maximum brightness in a dark-field image. An orientation matrix which describes the orientation of the crystal can be then calculated.

EBSD was conducted in a Quanta 600 field emission gun scanning electron microscope (FEG SEM) equipped with a TSL OIM™ system version 5.2. In the EBSD-determined inverse pole figure (IPF) maps presented below, gray and black lines indicate low-angle boundaries (LABs) and high-angle boundaries (HABs), respectively. Due to the limitations of EBSD, grain-boundary misorientations below 2° were excluded from the data analysis. Each non-indexed data point was automatically reassigned to the crystallographic orientation of its nearest neighbor in order to obtain a high fidelity picture of the microstructure. However, EBSD maps of heavily deformed titanium may contain a number of unsolved pixels. For example, approximately 70% of unsolved pixels after 90% cold rolling was reported in Ref. [14]. Therefore EBSD maps from specimens rolled to $\varepsilon_{th} = 2.66$ at both temperatures were excluded from consideration; however, some selected data from these trials were used for the purpose of calculations.

To determine post-rolling mechanical properties, tension tests were conducted at RT (for specimens rolled at both 293 and 77 K) and at 77 K (for specimens that had been subjected to cryorolling). For this purpose, flat specimens with gauge dimensions of 16 mm length × 3 mm width × 1.5 mm (or less, depending on the final sheet thickness following rolling) thickness were machined and pulled at a constant crosshead speed of $1\ mm\ min^{-1}$ in a screw-driven test machine to fracture. During tension testing at cryogenic temperature, the test specimen and both grips were immersed in an open-top vessel filled with liquid nitrogen whose level was continuously monitored and adjusted to ensure adequate temperature control.

3. Results

3.1. Microstructure and substructure evolution

In the as-received condition, the microstructure of the program material consisted of equiaxed grains with an average size of 15 μm (Fig. 1a). The grains contained no twins and essentially no internal substructure.

Rolling-plane, normal-direction (ND) IPF maps for CP Ti rolled at 293 and 77 K to a true thickness strain $\varepsilon_{th} = 0.16$, 0.36 or 0.92 are shown in Fig. 2. After rolling to $\varepsilon_{th} = 0.16$, a large number of twins were observed at

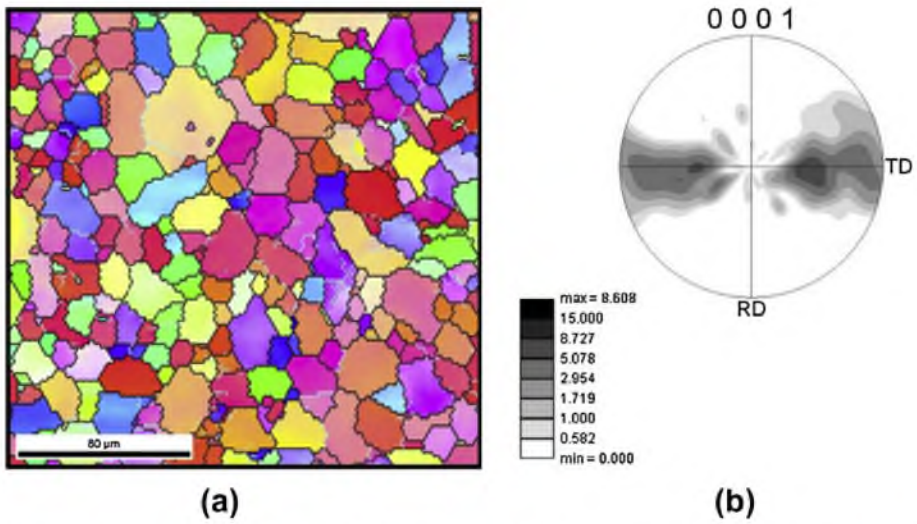

Fig. 1. ND EBSD (IPF) map taken from the rolling plane of the as-received CP Ti program material and the corresponding (0002) pole figure.

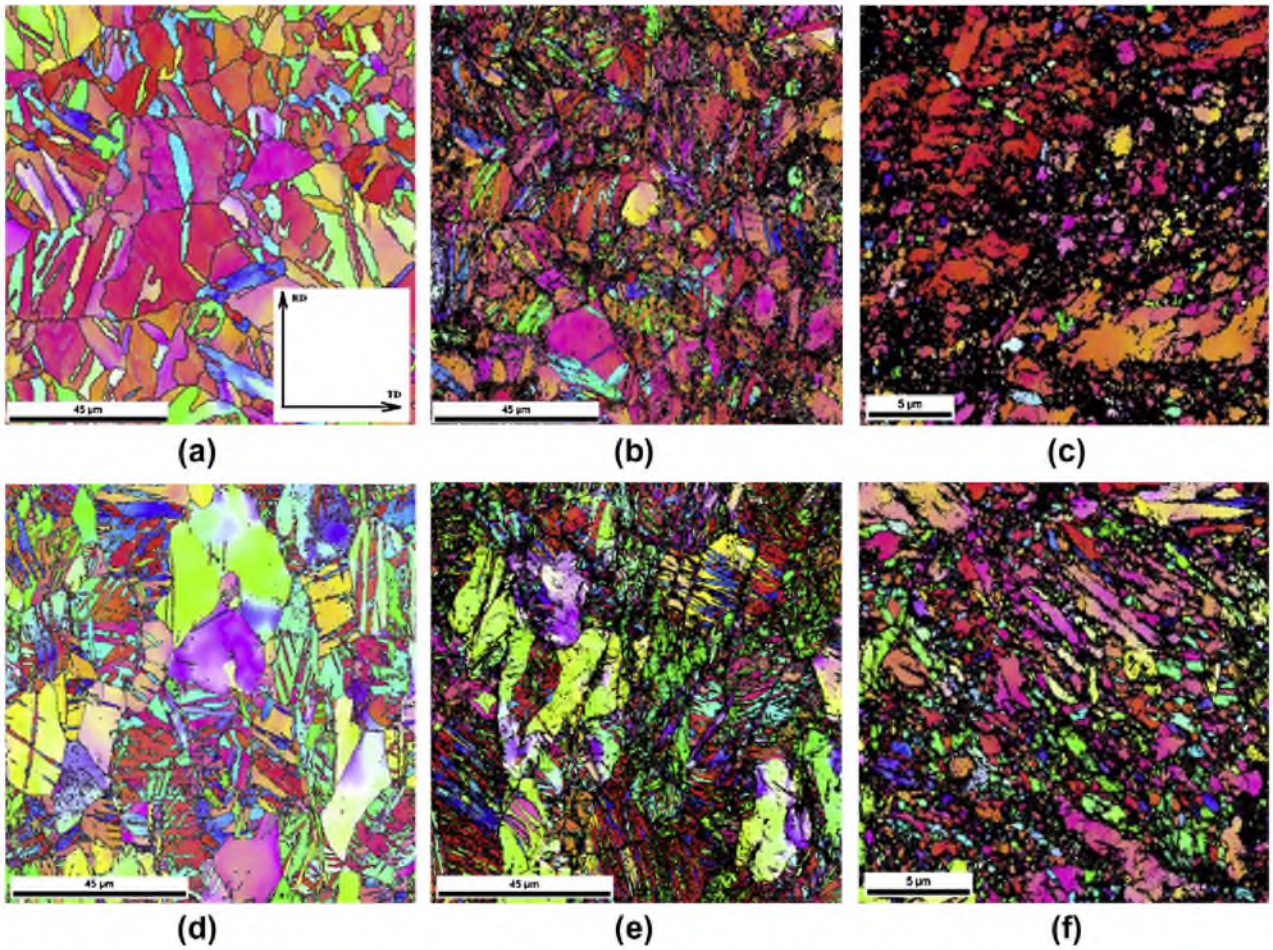

Fig. 2. ND EBSD (IPF) maps taken on the mid-thickness rolling plane of CP Ti samples rolled at (a–c) 293 K and (d–f) 77 K to true thickness strains ε_{th} of (a, d) 0.16, (b, e) 0.36 or (c, f) 0.92. All EBSD maps are shown in the as-scanned conditions for points with CI > 0.1.

both temperatures. However, the number of twins was noticeably greater and their thickness was smaller at the lower temperature (Fig. 2a and d). A number of intersecting twins from different systems and secondary twinning (within the primary twins) were observed in the microstructure of CP Ti rolled at 77 K to $\varepsilon_{th} = 0.16$ (Fig. 2d).

The number of twins increased after deformation to a thickness strain of 0.36 at both temperatures (Fig. 2b and

e). The interior of some grains after rolling at 77 K to $\varepsilon_{th} = 0.36$ appeared to have been almost completely consumed by twins (Fig. 2b). Rolling to a thickness strain of 0.92 at both temperatures resulted in the formation of a heterogeneous microstructure, consisting of grains with various degrees of twinning and areas with small grains. New grains were noticeably smaller for the case of the lower rolling temperature. At the same time, the number of black points (with a confidence index (CI) of less than 0.1) was larger after rolling at 77 K, thus implying a higher density of structural defects.

The corresponding results from TEM characterization are shown in Figs. 3 (RT) and 4 (77 K). Rolling at RT (293 K) to a thickness strain of $\varepsilon_{th} = 0.16$ resulted in the appearance of twins and a considerable dislocation density (Fig. 3a). The twins were distributed inhomogeneously in the microstructure, often appearing as clusters in various places. The mean thickness of the twins was 1.9–2.3 μm. With increasing strain, the twin thickness changed little while the spacing between them decreased noticeably, from 7.9 to 5.9 μm (Table 1). Dense dislocation walls and pile-ups were also observed. Further deformation to $\varepsilon_{th} = 0.92$ gave rise to a cellular microstructure with a high dislocation density (Fig. 3b). The boundaries of the cells were rather wide and loose. The size of the cells varied over a wide range from a hundred nanometers to a few micrometers. Individual subgrains with a size of 100–200 nm and thin clear boundaries were also observed. Rolling to $\varepsilon_{th} = 2.66$ at RT led to a considerable refinement of the microstructure and simultaneously to an increase in dislocation density (Fig. 3c and d). The size of cells was found to be approximately 200 nm. In addition, grains or subgrains with clear thin boundaries and a mean size of ~150 nm were also observed in the microstructure.

Rolling at 77 K resulted in a considerably denser structure of twins (Fig. 4a). In contrast to the behavior at RT, for which the twin thickness changed negligibly with strain, the mean thickness of twins decreased from 1.2 to 0.7 μm as the thickness strain increased from 0.1 to 0.36 (Table 1). This phenomenon was associated with the formation of new thinner twins with increasing strain rather than with the thinning per se of existing twins. Because the spacing between the twins also decreased from 3.5 to 2.8 μm over this interval of strain, "newer" twins might be expected to be thinner than the "older" ones. This effect can be detected in spite of fact that thicker "old" twins could exhibit slip-assisted growth due to dislocation reactions at twin interfaces and/or slip-independent growth due to direct activation of twin dislocations [18]. Microstructure evolution during further deformation was qualitatively similar to that found at RT. However, the microstructure developed at 77 K after $\varepsilon_{th} = 0.92$ was almost identical to that

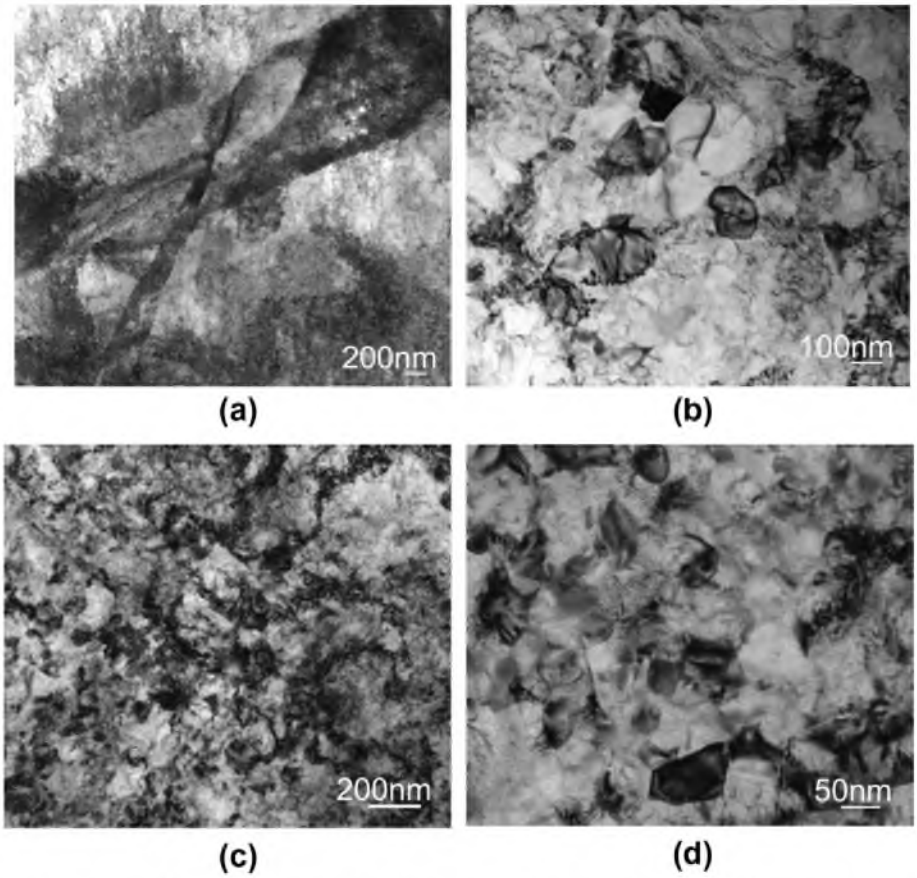

Fig. 3. TEM micrographs of CP Ti rolled at RT to a true thickness strain ε_{th} of (a) 0.16, (b) 0.92 or (c, d) 2.66.

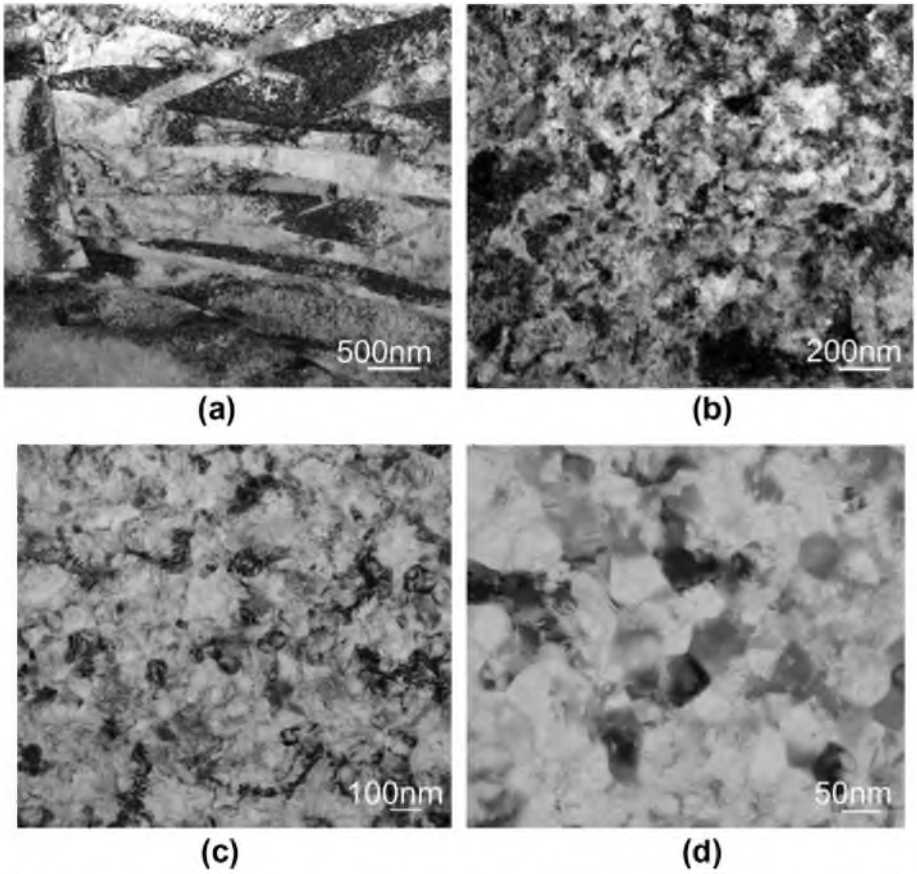

Fig. 4. TEM micrographs of CP Ti rolled at 77 K to a true thickness strain ε_{th} of (a) 0.16, (b) 0.92 or (c, d) 2.66.

Table 1
Twin thickness and spacing between twins as a function of thickness strain ε_{th} during rolling at 293 and 77 K.

ε_{th}	Twin thickness (μm)		Spacing between twins (μm)	
	293 K	77 K	293 K	77 K
0.1	2.3	1.2	7.9	3.5
0.22	1.9	1.0	6.5	3.0
0.36	2.2	0.7	5.9	2.8

obtained at 293 K after $\varepsilon_{th} = 2.66$ (Fig. 3c vs. 4b). Cryorolling to $\varepsilon_{th} = 2.66$ increased the homogeneity of the microstructure and decreased the grain/subgrain size slightly to ~80 nm (Fig. 4c and d).

Measurements of dislocation density showed a less pronounced development of dislocation substructure during the initial stages of cryorolling (Fig. 5). During RT rolling, the dislocation density in the matrix increased quickly at the initial stage of rolling (i.e. $\varepsilon_{th} \approx 0.2$), but then rose much more slowly during the rest of deformation (Fig. 5a). By contrast, the twins developed during RT rolling exhibited considerably more dislocations than the matrix. This observation supports the hypothesis that slip precedes twinning at RT and that twins engulf sessile dislocations that were previously glissile in the matrix [19].

Despite the confounding influence of scatter in the data, the dislocation density in the twins following rolling at 77 K was slightly higher than that in the matrix at the initial stages of deformation ($\varepsilon_{th} \leqslant 0.3$), and then the difference disappeared (Fig. 5b). Unlike the observations for room-temperature rolling, three stages were noted in the dislocation–density curves for both the matrix and the twins of cryorolled material (Fig. 5b). The first stage, characterized by a moderate rate of increase in dislocation density, was observed in the range $\varepsilon_{th} = 0$–0.35. During the second stage (for thickness strains of ~0.35–0.55), the dislocation density increased very rapidly. The third stage was associated with a nominally steady-state dislocation density.

Further examination of the data in Fig. 5 revealed that the dislocation density at the beginning of deformation at 77 K was almost three times lower than that that after comparable strains at RT. However, the dislocation densities in specimens rolled at both temperatures to $\varepsilon_{th} = 2.66$ were quite similar to each other. These observations suggest that early plastic deformation is mainly accommodated by twinning at 77 K and by slip at RT. Such a trend may perhaps be ascribed to the increase in the critical resolved shear stress for slip with decreasing deformation temperature [20].

Quantitative insight into the microstructure evolution was also obtained from EBSD measurements of the average grain size following rolling to various strain levels

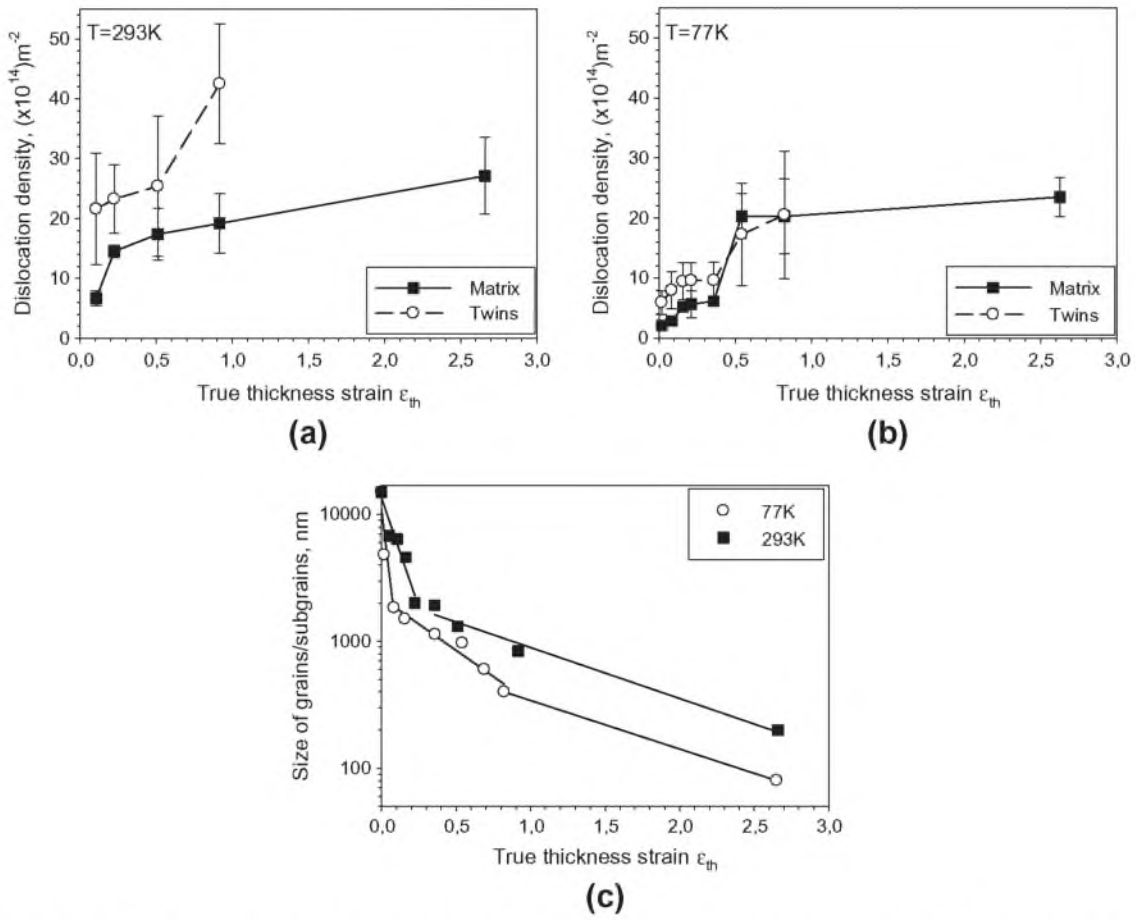

Fig. 5. Dislocation density in CP Ti samples as a function of thickness strain following rolling at (a) 293 K or (b) 77 K and (c) grain/subgrain size as a function of true thickness strain ε_{th} in CP Ti rolled at 293 and 77 K. The data for grain size in (c) were obtained by means of EBSD analysis (in the interval of $\varepsilon_{th} = 0$–0.92) and TEM ($\varepsilon_{th} = 2.66$).

($\varepsilon_{th} \leqslant 0.92$) at both temperatures (Fig. 5c); the EBSD measurements were supplemented by TEM observations for the largest strain (i.e. $\varepsilon_{th} = 2.66$). From a broad perspective, the rate of microstructure refinement was measurably greater in the case of deformation at 77 K (Fig. 5c). Moreover, the shapes of the two curves were noticeably different. Nevertheless, the grain size decreased very quickly with strain at both temperatures for $\varepsilon_{th} \leqslant 0.2$. These behaviors were obviously associated with twinning. In the interval of thickness strain between 0.2 and 0.35, the grain size during RT rolling did not change, most likely because of the saturation of twinning. During cryorolling, on the other hand, the grain size continued to decrease in the strain interval between 0.2 and 0.92, albeit at a lower rate than at lower strains. Deformation above $\varepsilon_{th} = 0.35$ at RT resulted in a gradual decrease in grain/subgrain size to 200 nm at $\varepsilon_{th} = 2.66$. Large deformation via cryorolling (to $\varepsilon_{th} = 2.66$) led to a greater degree of microstructure refinement and resulted in a grain/subgrain size of ~80 nm.

3.2. Twin characterization

Misorientation distributions (Fig. 6) showed several peaks in the high-angle region which could be identified with twin boundaries in the rolled CP Ti samples. After a thickness strain of 0.16 at RT (Fig. 6a), peaks corresponding to ~56, 64 and 86° were ascribed to the following respective twin families: (i) $(1\,0\,\bar{1}\,1)$ (57.42° around $\langle 2\,\bar{1}\,\bar{1}\,0\rangle$), (ii) $(1\,1\,\bar{2}\,2)$ (64.62° around $\langle 1\,0\,\bar{1}\,0\rangle$) and (iii) two different sets with similarly misoriented boundaries, viz. $(1\,0\,\bar{1}\,2)$ (84.78° around $\langle 2\,\bar{1}\,\bar{1}\,0\rangle$) and $(1\,1\,\bar{2}\,3)$ (86.98° around $\langle 1\,0\,\bar{1}\,0\rangle$). On the other hand, only two peaks (at 64 and 86°) were observed following rolling at 77 K. The same two peaks were observed during RT rolling to strains greater than $\varepsilon_{th} \approx 0.16$ (Fig. 6b and c). The height of the peaks associated with twinning decreased with strain at both temperatures, thus suggesting that the twinned areas lost coherency with the matrix due to large plastic deformation.

The misorientation results for the two lower strains also revealed a shallow peak at ~30° for both rolling temperatures (Fig. 6a and b). The appearance of this peak during deformation of hexagonal close-packed metals has been reported a number of times in the past (e.g. [14,21–23]). Most probably, it is associated with Σ13a coincident-site lattice boundaries (27.8° around $\langle 0001\rangle$). However, because this is neither a twin boundary nor a boundary between twin variants [24], the nature of its formation is still unclear [22,23].

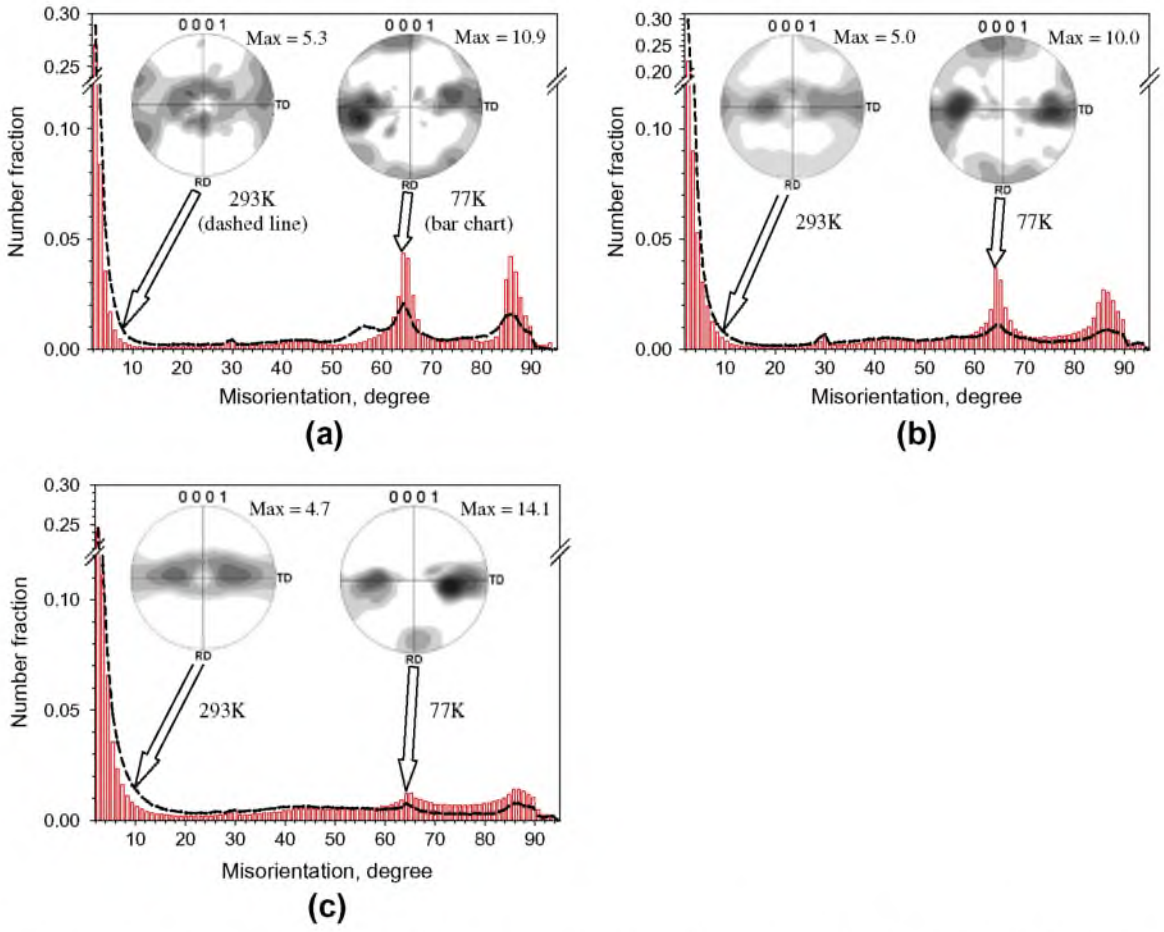

Fig. 6. Misorientation distributions and corresponding (0002) pole figures for CP Ti samples rolled at 293 or 77 K to a true thickness strain ε_{th} of (a) 0.16, (b) 0.36 or (c) 0.92. The pole-figure contour levels are shown in Fig. 1b.

The different extents of twinning during rolling at RT vs. 77 K are further quantified in Fig. 7a with the aid of EBSD analysis. Here, the aggregate fraction of twin boundaries among all of the high-angle boundaries is shown as a function of strain. The twin boundaries were categorized according to the Brandon criterion (calculated as $\Delta\theta = 15^\circ/\sqrt{\Sigma}$ relative to the perfect twin misorientation [25]). The maximum fraction of twin boundaries (~0.4) was similar for both rolling temperatures. However, the range of marked twin formation at 77 K ($\varepsilon_{th} \leqslant 0.2$) was found to be approximately twice the length of that at RT ($\varepsilon_{th} \leqslant 0.1$). During further deformation, the fraction of

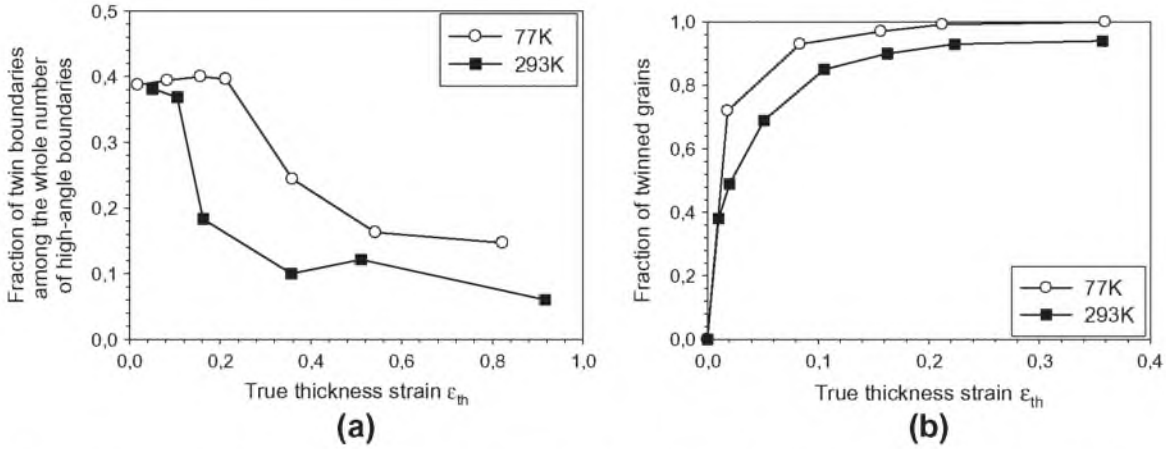

Fig. 7. Twin characteristics as a function of true thickness strain at 293 and 77 K: (a) EBSD-determined fraction of high-angle boundaries corresponding to twins; (b) fraction of twinned grains determined by optical microscopy.

twin boundaries meeting the Brandon criterion decreased quite rapidly at RT; a minimum value of ~0.1 was attained at $\varepsilon_{th} = 0.2$–0.3. During cryorolling, the fraction of boundaries with the twin misorientations decreased more slowly, attaining the value of ~0.16 at $\varepsilon_{th} \approx 0.5$.

Another metric of the more extensive twinning at the lower rolling temperature was the fraction of twinned grains (Fig. 7b). Specifically, the fraction of grains containing at least one twin reached 100% by $\varepsilon_{th} \approx 0.2$ during cryorolling, while the maximum fraction of twinned grains at RT was 0.93.

3.3. Texture evolution

The evolution of the overall crystallographic texture at both temperatures was typical for the cold rolling of CP Ti (e.g. [14]). Some imperfections in the EBSD-measured pole figures in comparison to ideal ones were associated with the relatively small areas that were scanned.

In the as-received condition (Fig. 1b), the (0002) pole figure consisted primarily of a split texture, with basal poles tilted ~30° from the ND toward the TD; weaker components were located ~80–90° from the ND toward the TD. Such pole figures are typical for hot-rolled titanium sheet products [26]. Texture evolution during rolling at RT to $\varepsilon_{th} = 0.16$–0.36 was associated with some weakening/splitting of the basal poles and the appearance of new weak peaks due to primary and secondary twinning [14] (Fig. 6a and b). By a thickness strain of 0.92, the influence of twinning on texture evolution had saturated, and the texture (Fig. 6c) had started to become similar to that observed in the initial condition.

After rolling at 77 K, the basal poles shifted somewhat more heavily toward the TD in comparison to the RT observations. In addition, the intensity of the texture increased relative to the initial condition and to the RT results. Moreover, new moderately strong (2–3 times random) poles were observed near the RD after cryorolling to $\varepsilon_{th} = 0.16$–0.36. These new peaks were associated with twinning. Unlike the results for RT deformation, twinning-induced peaks were observed even after $\varepsilon_{th} = 0.92$ at 77 K. In fact, the tilted basal poles had their maximum intensity after a thickness strain of 0.92.

3.4. Post-rolling tension testing

Typical true stress–true strain curves derived from load–stroke data prior to necking for tension testing of samples previously rolled at 77 or 293 K to various thickness strain ε_{th} are shown in Fig. 8. As noted in Materials and methods, the tension tests were conducted at the same temperature as the specific rolling trial, viz. 77 and 293 K (Fig. 8a and b). In addition, samples rolled at 77 K were then tension tested at 293 K (Fig. 8c) in order to elucidate the effect of temperature on the flow stress.

At cryogenic temperature (Fig. 8a), samples rolled to $\varepsilon_{th} \leqslant 0.36$ exhibited a steady increase in the true stress with strain and a relatively high uniform elongation of ~0.1–0.25. An increase in ε_{th} during cryorolling to 0.92 or 2.6 resulted in essentially the elimination of the strain hardening stage and early necking that is typical of severely cold-worked materials.

The tension test results for samples rolled and then tested at RT (Fig. 8b) were qualitatively similar to those for cryorolled and tension-tested samples. Principal differences comprised lower flow stress, strain-hardening rate and ductility for samples given light-to-moderate reductions ($\varepsilon_{th} = 0.05$–0.36). More heavily rolled Ti ($\varepsilon_{th} = 0.92$–2.6) had somewhat similar mechanical behavior during tension at both temperatures; however, the ductility was higher and the flow stress was lower after rolling at RT.

Differences in flow stress were not caused by different tension-test temperatures per se. In particular, the ultimate tensile strength of Ti rolled at 77 K and then pulled at RT was higher than that of material rolled and tension tested at RT. This behavior is most likely associated with the different microstructures formed by rolling at different temperatures. Furthermore, the influence of the as-rolled microstructure on the mechanical behavior of Ti during tension testing at RT increased with ε_{th}. However, the overall mechanical behavior in term of uniform elongation and work hardening rate of these two conditions was quite similar (Fig. 8b and c).

From an application standpoint, the maximum RT ultimate tensile strength of CP Ti after RT or cryorolling was ~900 and ~1100 MPa, respectively, or values which are very close to those of titanium alloys such as Ti-6Al-4 V.

4. Discussion

The results of the present work revealed the possibility of producing a high-strength nanostructure in titanium by cryorolling. As one of the main mechanisms of deformation, twinning plays an important role in the process of nanostructure formation and therefore merits detailed consideration.

The critical resolved shear stress (CRSS) for twinning in various metals and alloys depends weakly (if at all) on temperature compared to that for slip [24,27], as shown schematically in Fig. 9a. Denoting room and cryogenic temperatures as T and T_1, respectively, the figure suggests that the difference between the values of the CRSS for twinning and slip decreases with temperature from $\Delta\sigma_r$ to $\Delta\sigma_c$. The value of $\Delta\sigma_c$ may be very close to zero or even negative; i.e. the stress for twinning may be lower than that for slip. Hence, the onset of deformation at RT is generally associated with slip due to its lower critical resolved shear stress compared with that for twinning (e.g. [27]) (point A in Fig. 9a). The activation of twinning at RT occurs when the flow stress of the material increases due to strain hardening and the resolved shear stress reaches point B, which corresponds to the onset of Stage B hardening in Ref. [19]. At the lower (cryogenic) temperature, the value of $\Delta\sigma_c$

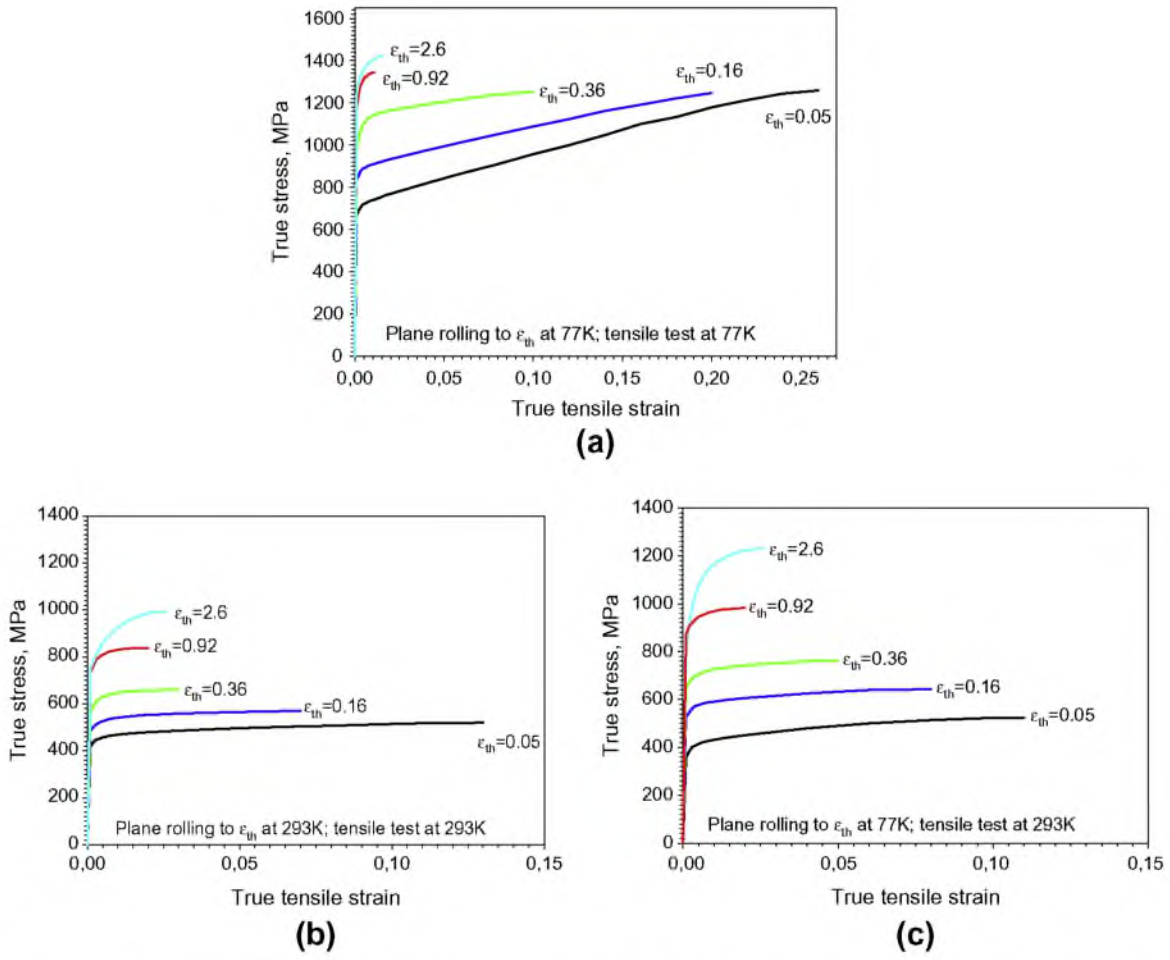

Fig. 8. True stress–true strain curves for the CP Ti rolled at (a, c) 77 K or (b) 293 K to a true thickness strain between 0.05 and 2.6. The temperature of the tension test was (a) 77 K or (b, c) 293 K. The true thickness strain imposed during rolling prior to tension testing is indicated in the figures.

(between Λ_1 and B_1) is much smaller, and therefore slip and twinning may be activated at approximately the same time.

The preference for the activation of slip vs. twinning at each temperature depends on microstructural parameters as well, however. With a decrease in grain size, the CRSS for twinning increases more rapidly than that for slip. Ignoring the effect of prior stored work and strain-path change on the yield strength and assuming a yield-strength dependence on grain size following Hall–Petch-type relationships, $\sigma = \sigma_0 + kd^{-1/2}$, the slope k_t for twinning is generally higher than the slope k_s for slip (Fig. 9b) [27–29]. During rolling, deformation twinning refines the microstructure of Ti noticeably (Fig. 5c), thereby increasing the flow stress of the material. As a result, slip becomes preferable and twinning is suppressed as the grain size is reduced below d or d_1 (Fig. 9b). The results of the present work indicate that a decrease in rolling temperature extends the twinning stage to a smaller grain size (Fig. 7). Therefore, the inflection point should shift to a smaller grain size with a decrease in temperature from T to T_1. That is to say, d_1 (corresponding to 77 K) must be smaller than the value of d pertinent to RT deformation.

The yield-strength results of the present work are in qualitative agreement with this kind of reasoning (Fig. 9c). At both temperatures, the curves exhibited a bilinear behavior comprising a large initial slope and a smaller slope at larger values of $d^{-1/2}$. The trend lines corresponding to tension testing at 77 K following cryorolling were much higher than those for RT rolling/tension testing. At RT, the inflection point occurred at a grain size of 0.8–0.9 μm; for cryorolled samples, the inflection point was observed at $d \approx 0.6$ μm.

The contribution of the various strengthening mechanisms to the overall yield strength σ_y can be typically expressed as $\sigma_y = \sigma_0 + \sigma_\rho + \sigma_{H\text{-}P}$, in which σ_0 denotes the friction stress, σ_ρ is the substructure strengthening due to dislocation density and low-angle boundaries, and $\sigma_{H\text{-}P}$ is the Hall–Petch strengthening. Some additional microstructural parameters, such as those which quantify the transition of dislocations from glissile to sessile configurations within the twins (Basinski hardening) and texture-induced hardening/softening due to the crystal rotations associated with twinning [19] and slip, also influence on the strength level of the material.

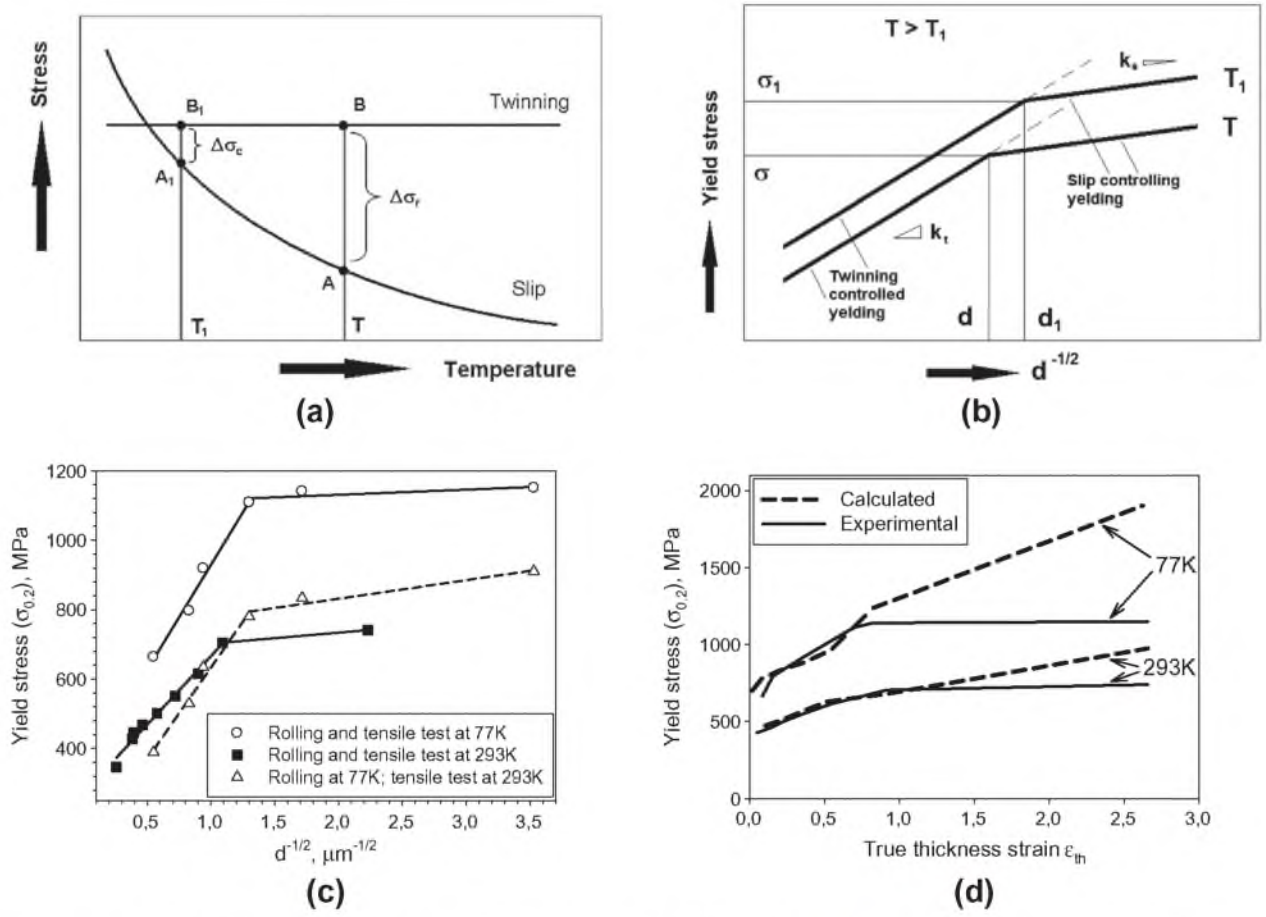

Fig. 9. Schematic illustrations showing (a) the effect of temperature on the deformation mode [27] and (b) the effect of microstructure refinement on the yield stresses at different temperatures [24,29]. The measured relationship between grain/subgrain size and flow stress at 0.2% strain is shown in (c), and the comparison between the calculated and experimental values of yield stress for CP Ti samples rolled at 293 and 77 K to various thickness strains is presented in (d).

According to Ref. [8], the substructure strengthening σ_ρ can be expressed as $\sigma_\rho = M\alpha Gb\sqrt{\frac{1.5S_v\theta_{LAB}}{b} + \rho}$, in which M is the Taylor factor; α is a constant in the range of 0.05–1 [30,31]; G is the shear modulus; b is the Burgers vector; S_v is the boundary area per unit volume; θ_{LAB} is the average misorientation of low-angle boundaries; and ρ is the dislocation density. The texture hardening/softening effects due to twinning and slip were estimated via the Taylor factor M, which was determined for uniaxial tension along the RD direction using TSL OIM™ software assuming the ratio of the critical resolved shear stresses for prism$\langle a\rangle$:basal$\langle a\rangle$:pyramidal$\langle c+a\rangle$ slip to be 0.75:1:4 [32].

The nature of Basinski hardening is associated with the density of sessile and glissile dislocations within twins. Reorientation of the lattice due to twinning immobilizes glissile dislocations produced prior to twinning. In order to ensure the deformability of the interior of the twins, therefore, new dislocations are produced, thus increasing the overall dislocation density (especially in the case of RT, Fig. 5) and hence the strength of the twinned regions due to dislocation interactions [33]. The contribution of the Basinski hardening can be estimated via the dislocation density within the twins. The overall dislocation density in the present work was calculated as $\rho = \rho_t(f_t) + \rho_m(1 - f_t)$, where ρ_t and ρ_m are dislocation density in twins (sessile and glissile) and matrix, respectively and f_t is the volume fraction of twins.

The Hall–Petch contribution to the yield strength/flow stress is typically of the form $\sigma_{H-P} = \frac{K_y}{\sqrt{d}}$, in which K_y is the slope of the straight line relating the yield stress of polycrystalline material to the inverse square root of grain size d.

Estimates of the flow stress as a function of imposed rolling strain made use of the data in Table 2 and the following parameters: $\alpha = 0.05$; $G = 4.36 \times 10^{10}$ N m^{-2} or 4.95×10^{10} N m^{-2} for $T = 293$ and 77 K, respectively [34]; and $b = 2.95 \times 10^{-10}$ m [34]. The value of S_v for both temperatures was determined via EBSD as $(4/\pi)L_A$ [35], in which L_A denotes the total low-angle boundary length per unit of scan area [15] (Table 2). The average misorientation of low-angle boundaries at both temperatures was also drawn from the results of EBSD analysis (Table 2). The dislocation density in the matrix and twins was taken from Fig. 5a and b; f_t was taken as the ratio of twin boundaries

Table 2
Input data for the calculation of the yield stress ($\sigma_{0.2}$) and specific strengthening contributions (σ_ρ, $\sigma_{H\text{-}P}$) as a function of thickness strain ε_{th} during rolling of commercially pure titanium at 293 and 77 K.

Rolling temperature	293 K					77 K				
ε_{th}	0.1	0.2	0.5	0.9	2.6	0.1	0.2	0.5	0.9	2.6
M	4.02	3.72	4.45	4.45	4.6	4.43	4.12	4.15	4.71	4.69
L_A (m^{-1})	11.5	1144.0	2516.3	3033.4	2887.3	378.9	728.3	2285.2	4301.3	7012.1
θ_{LAB} (radian)	0.066	0.063	0.069	0.08	0.087	0.062	0.061	0.065	0.067	0.085
σ_ρ (MPa)	151.1	162.3	174.8	193.8	208.0	107.6	125.8	196.3	203.4	221.0
$\sigma_{H\text{-}P}$ (MPa)	92.9	127.4	213.6	256.4	525.46	248.2	293.9	365.5	617.4	1270.8

length to the total length of high-angle boundaries (Fig. 7a). The grain size d was taken from Fig. 5c. The values of σ_0 were experimentally determined as the yield stress of the program material in the β-annealed and furnace-cooled condition (grain size ~1000 μm): at 293 K, $\sigma_0 = 290$ MPa; at 77 K, $\sigma_0 = 460$ MPa. The values of K_y for both temperatures were taken from [20]: at 293 K, $K_y = 0.24$ MN $m^{-3/2}$; at 77 K, $K_y = 0.36$ MN $m^{-3/2}$.

The results of the calculations in terms of yield stress as a function of imposed true thickness strain at 293 and 77 K are compared with the experimental curves in Fig. 9d. The predictions mirrored the experimental results for ε_{th} between 0 and ~1. However, the large strain portion of the predicted curves deviated considerably from the experimental curves; the differences for $\varepsilon_{th} = 2.6$ were 32 and 65% at 239 and 77 K, respectively. As discussed above with respect to Fig. 9b and c, such large deviations can be ascribed to changes in the value of K_y with strain/grain refinement [27–29]. Improved agreement at large values ε_{th} can be attained assuming $K_y = 0.13$ MN $m^{-3/2}$ for 293 K and 0.18 MN $m^{-3/2}$ for 77 K, i.e. decreasing K_y by a factor of approximately two in both cases for ε_{th} above ~0.9. This result is in reasonable agreement with the data tabulated in Ref. [27].

It may thus be concluded that twinning plays a crucial role during the first stage of microstructure evolution. However, as soon as the size of stable grains/subgrains becomes smaller than the average thickness of the twins or the spacing between the twin boundaries (Table 1), twinning and twin interactions per se should not be considered the mechanism of strengthening/microstructure refinement. According to Ref. [36], the minimum grain size at which twinning still can operate at RT is $d \sim 0.7$ μm, which is in good agreement with the results of the present work.

The rate of the microstructure formation and the size of subgrains/grains during further rolling depend on the strain hardening/dynamic recovery relationship at room or cryogenic temperature. In the case of cryorolling, a higher strain hardening rate (initially due to the rapid generation of twins and then due to the rapid increase in dislocation density) combined with slower dynamic recovery increases the flow stress of Ti to a very high level (Fig. 8a). In accordance with the well-known empirical relationship between the flow stress and the steady-state grain size during deformation, $\sigma \sim d^{-m}$, in which $m < 1$ [37,38], the high level of the flow stress should result in a smaller grain size in comparison with RT behavior. Indeed, the results of the present work show a decrease in grain/subgrain size from ~200 to ~80 nm when the deformation temperature is decreased from 293 to 77 K. However, the decrease in deformation temperature does not change the physics of the microstructure formation but, rather, increases the kinetics of the process, thereby decreasing the size of grains to the nanoscale.

5. Conclusions

Microstructure evolution during plane-strain rolling of commercial-purity titanium at 77 and 293 K was investigated. The following conclusions can be drawn from this work:

1. Microstructure evolution in CP Ti during rolling at both temperatures (77 and 293 K) was associated with twinning, following by the formation of high-angle deformation-induced boundaries. At 77 K, twinning was more extensive in terms of the fraction of twinned grains and the range of strain over which twinning occurred.
2. The mechanical behavior of titanium during rolling at each temperature can be described by a bilinear Hall–Petch-type relationship. With a decrease in grain size due to twinning to 0.8–0.9 μm at 293 K or to 0.6 μm at 77 K, the slope k_y decreases by a factor of ~2 for both temperatures. Using strain-dependent values of k_y, the contributions of the main strengthening factors (grain size, substructure, texture change due to slip and twinning) can be quantified in an approximate fashion.
3. Rolling to a true thickness strain of 2.66 resulted in the formation of a microstructure with a grain size of ~80 or 200 nm at 77 or 293 K, respectively, and an ultimate tensile strength of 1100 or 900 MPa at 77 or 293 K, respectively.

Acknowledgement

This work was supported by the Federal Agency for Education, Russia; Grant #14.A18.21.0439.

References

[1] Meyers MA, Mishra A, Benson DJ. Prog Mater Sci 2006;51:427.

[2] Kumar KS, Van Swygenhoven H, Suresh S. Acta Mater 2003;51:5743.
[3] Zhilyaev AP, Langdon TG. Prog Mater Sci 2008;53:893.
[4] Valiev RZ, Langdon TG. Prog Mater Sci 2006;51:881.
[5] Tsuji N, Saito Y, Utsunomiya H, Tanigawa S. Scripta Mater 1999;40:795.
[6] Beygelzimer Y, Varyukhin V, Synkov S, Orlov D. Mater Sci Eng A 2009;503:14.
[7] Zherebtsov SV, Salishchev GA, Galeyev RM, Valiakhmetov OR, Mironov SYu, Semiatin SL. Scripta Mater 2004;51:1147.
[8] Hughes DA, Hansen N. Acta Mater 2000;48:2985.
[9] Belyakov A, Sakai T, Miura H, Tsuzaki K. Philos Mag A 2001;81:2629.
[10] Rybin VV. Severe plastic deformation and fracture of metals. Moscow: Metallurgy Press; 1986 [in Russian].
[11] Ivanisenko Yu, Lojkowski W, Valiev RZ, Fecht H-J. Acta Mater 2003;51:5555.
[12] Hansen N, Jensen DJ. Philos Trans Roy Soc Lond A 1999;357:1447.
[13] Salishchev G, Mironov S, Zherebtsov S, Belyakov A. Mater Charact 2010;61:732.
[14] Chun YB, Yu SH, Semiatin SL, Hwang SK. Mater Sci Eng A 2005;398:209.
[15] Zherebtsov SV, Dyakonov GS, Salem AA, Malysheva SP, Salishchev GA, Semiatin SL. Mater Sci Eng A 2011;528:3472.
[16] Moskalenko VA, Smirnov AR, Moskalenko AV. Low Temp Phys 2009;35:905.
[17] Valiev RZ, Vergazov AN, Gertsman VY. Crystallogeometric analysis of intercrystalline boundaries in the practice of electron microscopy. Moscow: Nauka Pub.; 1991.
[18] Capolungo L, Beyerlein IJ, Tomé CN. Scripta Mater 2009;60:32.
[19] Salem AA, Kalidindi SR, Doherty RD, Semiatin SL. Metall Mater Trans A 2006;37:259.
[20] Conrad H. Prog Mater Sci 1981;26:123.
[21] Zherebtsov S, Lojkowski W, Mazur A, Salishchev G. Mater Sci Eng A 2010;527:5596.
[22] Mironov SYu, Myshlyaev MM. Phys Solid State 2007;49:858.
[23] Ostapovets A, Seda P, Jager A, Lejcek P. Scripta Mater 2011;64:470.
[24] Stanford N, Carlson U, Barnett MR. Metall Mater Trans A 2008;39:934.
[25] Brandon DG. Acta Metall 1966;14:1479.
[26] Zwicker U. Titanium and titanium alloys. Berlin: Springer; 1974.
[27] Meyers MA, Vohringer O, Lubarda VA. Acta Mater 2001;49:4025.
[28] Hull D. Acta Metall 1961;9:191.
[29] Barnett MR. Scripta Mater 2008;59:696.
[30] Hall D, Bacon DJ. Introduction to dislocations. 3rd ed. Oxford: Butterworth-Heinemann; 1984.
[31] Kozlov EV, Koneva NA. Mater Sci Eng A 1997;234–236:982.
[32] Salem AA, Kalidindi SR, Semiatin SL. Acta Mater 2005;53:3495.
[33] Hirth JP, Lothe J. Theory of dislocations. New York: Wiley; 1982.
[34] Frost HJ, Ashby MF. Deformation-mechanism maps: the plasticity and creep of metals and ceramics. Oxford: Pergamon Press; 1982.
[35] ASM Handbook. Metallography and microstructure, vol. 9. Materials Park, OH: ASM International; 1992.
[36] Yu Q, Shan Z-W, Li J, Huang X, Xiao L, Sun J, et al. Nature 2010;463:335.
[37] Humphreys F, Hatherly M. Recrystallization and related annealing phenomena. 2nd ed. Oxford: Elsevier; 2004.
[38] Dudova N, Belyakov A, Sakai T, Kaibyshev R. Acta Mater 2010;58:3624.